Acta Crystallographica Section D
Biological Crystallography
ISSN 0907-4449

Preliminary neutron diffraction studies of *Escherichia coli* dihydrofolate reductase bound to the anticancer drug methotrexate

Brad C. Bennett,[a] Flora Meilleur,[b] Dean A. A. Myles,[b,c] Elizabeth E. Howell[a] and Chris G. Dealwis[a]*

[a]Department of Biochemistry, Cellular and Molecular Biology, University of Tennessee–Knoxville, Knoxville, TN, USA, [b]Institut Laue–Langevin, Grenoble, France, and [c]Center for Structural Molecular Biology, Oak Ridge National Laboratory, Oak Ridge, TN, USA

Correspondence e-mail: cdealwis@utk.edu

Received 2 December 2004
Accepted 10 February 2005

The contribution of H atoms in noncovalent interactions and enzymatic reactions underlies virtually all aspects of biology at the molecular level, yet their 'visualization' is quite difficult. To better understand the catalytic mechanism of *Escherichia coli* dihydrofolate reductase (ecDHFR), a neutron diffraction study is under way to directly determine the accurate positions of H atoms within its active site. Despite exhaustive investigation of the catalytic mechanism of DHFR, controversy persists over the exact pathway associated with proton donation in reduction of the substrate, dihydrofolate. As the initial step in a proof-of-principle experiment which will identify ligand and residue protonation states as well as precise solvent structures, a neutron diffraction data set has been collected on a 0.3 mm^3 D_2O-soaked crystal of ecDHFR bound to the anticancer drug methotrexate (MTX) using the LADI instrument at ILL. The completeness in individual resolution shells dropped to below 50% between 3.11 and 3.48 Å and the $I/\sigma(I)$ in individual shells dropped to below 2 at around 2.46 Å. However, reflections with $I/\sigma(I)$ greater than 2 were observed beyond these limits (as far out as 2.2 Å). To our knowledge, these crystals possess one of the largest primitive unit cells ($P6_1$, $a = b = 92$, $c = 73$ Å) and one of the smallest crystal volumes so far tested successfully with neutrons.

1. Introduction

Dihydrofolate reductases (DHFRs) are conserved across species from archaea to the higher mammals (Kraut & Matthews, 1987) and are critical for multiple metabolic pathways, including pyrimidine and amino-acid biosynthesis as well as other processes involving one-carbon transfer reactions (for an excellent review, see Schnell *et al.*, 2004). They catalyze the NADPH-dependent reduction of 7,8-dihydrofolate (DHF) to 5,6,7,8-tetrahydrofolate (THF). The importance of this step lies in the partial recycling of the THF metabolite N^5-N^{10}-methylene-THF, which serves to donate a methyl group to deoxyuridylmonophosphate (dUMP), thus converting dUMP to deoxythymidylmonophosphate (dTMP). The dTMP nucleotides are then incorporated into DNA at the S phase or during DNA-damage response. Another product of the methyl-transfer reaction is DHF, the substrate for DHFR (Kraut & Matthews, 1987). The ability to block the catalytic activity of DHFR leads to interruption of DNA synthesis, genomic instability and ultimately cell death. Accordingly, several therapeutic agents have been discovered that can inhibit DHFR, most notably the antitumor drugs aminopterin and amethopterin (or methotrexate; MTX) and the antimicrobial trimethoprim (TMP; Huennekens, 1994, 1996; Schnell *et al.*, 2004).

There are more than 45 X-ray structures available for ecDHFR in 28 different liganded states as deposited in the PDB (http://www.rcsb.org; Berman *et al.*, 2000). The overall three-dimensional structure of DHFR is dominated by a central eight-stranded β-sheet, with the upper four sheets maintaining the nucleotide- or cofactor-binding domain while the lower ones maintain the substrate-binding or loop domain (Bolin *et al.*, 1982; Bystroff *et al.*, 1990; Matthews *et al.*, 1977; Reyes *et al.*, 1995). The substrate and cofactor bind at a cleft formed at the interface of the two domains and the positioning of one of the loops, the M20 loop (residues 9–24), has been proposed to be linked to the positioning of the enzyme along the reaction coordinate (Miller & Benkovic, 1998; Miller *et al.*, 2001; Sawaya & Kraut, 1997).

The active site of ecDHFR is quite hydrophobic, with the only ionizable residue being Asp27, which is positioned upon α-helix *B* framing the back of the active site (Bolin *et al.*, 1982; Matthews *et al.*, 1977, 1985). The protonation state of Asp27 is the subject of great controversy. Early crystallographic studies of DHFR bound to DHF analogs (such as MTX) revealed that the active site Asp27 is actually >5 Å away from the N5 atom on the pteridine ring of the substrate (Bolin *et al.*, 1982; Matthews *et al.*, 1977; Reyes *et al.*, 1995). Mutagenesis studies in which the Asp27 was replaced by Ser or Asn show a severe decrease in catalytic rate and efficiency (Howell *et al.*, 1986; Villafranca *et al.*, 1983). How Asp27 is involved in catalysis is therefore of great interest and a number of groups have proposed different roles for this residue. Whilst initial mutagenesis studies suggested that Asp27 serves as a general acid, later studies proposed that Asp27 acts by elevating the N5 pK_a of bound DHF from 2.59 to 6.5, using long-range polarization effects to induce and maintain protonation of DHF once bound (Bajorath *et al.*, 1991; Chen *et al.*, 1994, 1997). Since a pH profile of ecDHFR reveals a catalytic pK_a for the hydride-transfer step of 6.5 (Fierke, Johnson *et al.*, 1987), this titration could correlate with a perturbed pK_a for either Asp27 or DHF. Recent ^{13}C NMR studies have shown that the homologous Asp26 residue in *Lactobacillus casei* DHFR possesses a pK_a of less than 4, so this residue appears to be negatively charged at physiological pH (Casarotto *et al.*, 1999). Additionally, a resonance Raman study has established the pK_a of the N5 on DHF to be 6.5 when bound to ecDHFR in a ternary complex with NADP$^+$ (Chen *et al.*, 1994), whereas more recent Raman difference spectra reveal that the Asp27 probably has a pK_a of below 5 and thus is charged, at least in the ground state (Chen *et al.*, 1997). This suggests that the kinetic pK_a observed relates to the protonation state of the bound ligand and not the Asp27 residue. Using computational approaches, various groups have proposed different pathways of proton donation and different ionization states for Asp27 and bound ligands (Bajorath *et al.*, 1991; Cannon *et al.*, 1997; Chen *et al.*, 1997; Greatbanks *et al.*, 1999).

In contrast to the catalytic protonation mechanism, evidence from X-ray crystallography, NMR and difference spectra suggest that the N1 atom of MTX is protonated and thus positively charged when bound to ecDHFR (Appleman *et al.*, 1988; Bolin *et al.*, 1982; Cocco *et al.*, 1981, 1983; Hood & Roberts, 1978; London *et al.*, 1986; Matthews *et al.*, 1977; Ozaki *et al.*, 1981; Poe *et al.*, 1972). The binding of MTX in the DHFR active site is such that the N1 atom is within 2.6–2.7 Å of Asp27 O$^{\delta 2}$, stemming from an orientation of the pteridine ring which is flipped compared with folate and DHF binding, a consequence of a 180° rotation about the C6—C9 bond. The close proximity of N1 of MTX when bound to DHFR to the Asp27 carboxylate group strongly suggests a hydrogen-bonding interaction. This interaction is seemingly so favorable that the N1 pK_a increases from 5.7 for free MTX to >10 for DHFR-bound MTX (Cocco *et al.*, 1983) and is hypothesized to be the reason that the dissociation constants for folate and DHF for ecDHFR are so much higher than for MTX (Appleman *et al.*, 1988; Stone & Morrison, 1988). A recent computational study proposes that Asp27 is protonated while MTX is neutral while bound to ecDHFR; therefore, the interaction is suggested to be dipole–dipole rather than ionic (Cannon *et al.*, 1997). Direct determination of hydrogen positions within the active site of ecDHFR has not been demonstrated and the lack of a consensus on ecDHFR's mechanism of proton donation arises from the seemingly simple and related question: what are the protonation states of Asp27 and bound ligands in the ecDHFR active site?

Single-crystal diffraction by neutrons can reveal the positions of H atoms, especially the deuterium isotope, at moderate resolution (2.5–2.0 Å and beyond). These have included studies on concanavalin A (ConA; Blakeley *et al.*, 2004; Habash *et al.*, 1997, 2000), endothiapepsin (Cooper & Myles, 2000; Coates *et al.*, 2001), rubredoxin (Chatake *et al.*, 2004; Kurihara *et al.*, 2004), xylose isomerase (Hanson *et al.*, 2004) and myoglobin (Ostermann *et al.*, 2002; Shu *et al.*, 2000). Incoherent scattering of hydrogen gives rise to higher background in neutron diffraction experiments, which can be overcome in part by H/D solvent exchange and more completely by preparing perdeuterated material, which results in a significant improvement in signal-to-noise ratio (Schoenborn & Knott, 1996; Tuominen *et al.*, 2004).

In order to identify hydrogen positions within the ecDHFR active site and on bound methotrexate, we have produced D_2O-soaked ecDHFR–MTX crystals suitable for preliminary neutron diffraction analysis and a partial data set has been collected at room temperature at the Institut Laue–Langevin (ILL). The completeness in individual resolution shells dropped to below 50% between 3.11 and 3.48 Å and the $I/\sigma(I)$ in individual shells dropped to below 2 at around 2.46 Å. However, reflections with $I/\sigma(I)$ greater than 2 were observed beyond these limits and some were observed as far out as 2.2 Å.

2. Materials and methods

2.1. Expression, purification and crystallization of the ecDHFR–MTX complex

ecDHFR was purified from the SK383 strain of *Escherichia coli* (Zeig *et al.*, 1978) that contains a pUC8 plasmid encoding the gene for expression of ecDHFR (Bystroff *et al.*, 1990). The

SK383 *E. coli* strain was grown in Terrific Broth in the presence of ampicillin. Expression of ecDHFR was constitutive, not induced, and the cells were grown by shaking at 250 rev min^{-1} at 310 K for ~72 h. The cells were then harvested by centrifugation, flash-frozen in liquid nitrogen and stored at 193 K until ready for purification. A complete purification protocol can be found elsewhere (Poe *et al.*, 1972; Taira *et al.*, 1987). Briefly, ecDHFR was purified using a two-step procedure involving an MTX inhibitor affinity column (Sigma Chemical Co., MO, USA) and a DEAE-Sephacel weak anion-exchange column (Pharmacia, NJ, USA). After the affinity column, ecDHFR is >90% pure. The ion-exchange step removes folate, the competitive ligand used to elute ecDHFR from the MTX affinity column. The yield of pure ecDHFR is normally 12–15 mg per litre of TB media.

The protein was concentrated to 0.75–1.5 mg ml^{-1} with an Amicon YM10 membrane-filtration device (Millipore, MA, USA) before adding the ligand. Because of its relative insolubility at high concentrations, the MTX is added (as a solid and at a fivefold molar ratio) while the protein is relatively dilute. After a short incubation with MTX, ecDHFR was then concentrated with a Centricon YM10 (Millipore, MA, USA) device until the volume was one-tenth of the starting volume. It was then rediluted back to the starting volume with crystallization buffer [0.1 *M* Tris–HCl pH 7, 2 m*M* dithioerythritol (DTE) and a trace amount of MTX] and reconcentrated in the same manner. This step was repeated twice. To generate large-volume DHFR crystals for neutron diffraction, it is necessary to maximize crystal growth with minimal nucleation points within the drop while using highly concentrated protein. To achieve this, we ultimately concentrated ecDHFR to >50 mg ml^{-1} and set up large drops at >50 µl total volume in a modified sitting-drop format using optimized precipitant and salt conditions. Moderate- to large-sized crystals (a few grew to 1.4 × 1.0 × 0.3 mm) were grown at 277 K by mixing equal volumes (25 µl) of the protein complex with the reservoir buffer, 0.1 *M* Na HEPES pH 7.5, 0.2 *M* $CaCl_2$ and 18%(*v*/*v*) PEG 400 (optimized from a condition in Hampton Crystal Screen No. 1, Hampton Research, CA, USA; Jancarik & Kim, 1991) on siliconized cover slips and placing them on a Plexiglas support. Pyrex (Corning, NY, USA) custard dishes were used as the reservoirs (40 ml total volume of mother liquor) with the support sitting in the dish and the whole apparatus was sealed by a thick circle of Plexiglas, using vacuum grease (Dow Corning, MI, USA) to finish the seal. Crystals appeared in 1 d and grew to full size in about two weeks.

2.2. D_2O-soaking and harvesting of crystals for neutron diffraction experiments

Several ecDHFR/MTX crystals were subjected to H/D exchange prior to neutron data collection in order to reduce the large hydrogen incoherent scattering contribution to the background. To prevent 'shocking' the crystals, they were H/D-exchanged conservatively against an increasing gradient of D_2O-based crystallization buffer [0.1 *M* Na HEPES pH 7.5 from a 1 *M* buffer stock made with D_2O, 0.2 *M* solid $CaCl_2$ and 18%(*v*/*v*) PEG 400, all components dissolved in D_2O] over the course of one week (*i.e.* from an initial ratio of 10% D_2O/90% H_2O, the D_2O% concentration was doubled every other day until 90–100% D_2O content was achieved). After one month, the crystals were mounted into custom-prepared quartz capillaries with a 2.9 mm outer diameter (Vitrocom, Inc., NJ, USA) with a D_2O 'plug' at one end, sealed at both ends with epoxy and paraffin wax and stored securely in a sealed 50 ml Falcon tube at 277 K for transport and for storage until data collection. The crystal mounting was performed in a D_2O-saturated environment: a tent was erected in a 277 K room with N_2-purged D_2O pumped into the tent to prevent back-exchange of crystal and buffer ^2H atoms with ^1H in H_2O vapor in the environment. The dimensions of the crystal used for neutron data collection were 1.4 × 1.0 × 0.3 mm. Owing to the hexagonal external morphology of these crystals (*i.e.* they are not a perfect cubic shape), we estimate the volume of this crystal to be 0.3 mm^3.

Table 1
Neutron diffraction data statistics for ecDHFR–MTX.

Obtained at the Institut Laue–Langevin (ILL) neutron source. Values in parentheses are for the highest resolution shell.

Instrument	LADI
Wavelength range used (quasi-Laue) (Å)	2.80–3.70
Resolution range (Å)	25.0–2.20 (2.32–2.20)
Space group	$P6_1$
Unit-cell parameters (Å, °)	a = 90.93, b = 90.93, c = 72.36, α = 90, β = 90, γ = 120
Total measured reflections	17091 (1302)
Total unique reflections	7511 (824)
Completeness (%)	43.9 (33.3)
Multiplicity	2.3 (1.6)
$I/\sigma(I)$	2.6 (2.0)
Mean $I/\sigma(I)$	4.3 (3.0)
$R_{\rm merge}$† (%)	20.6 (26.4)

† $R_{\rm merge} = \sum_{hkl}\sum_i |I_i(hkl) - I_{hkl}| / \sum_{hkl}\sum_i I(hkl)$.

Table 2
Data-reduction statistics (calculated using *SCALA*).

$d_{\rm min}$ (Å)	$R_{\rm merge}$	$R_{\rm cum}$	$I/\sigma(I)$	Mn(I)/sd	Poss† (%)	CumPoss‡ (%)	Multiplicity
6.96	0.160	0.160	4.0	6.5	85.3	85.3	3.3
4.92	0.186	0.175	3.7	6.3	84.1	84.5	3.5
4.02	0.193	0.182	3.5	5.8	78.1	81.6	3.2
3.48	0.198	0.185	3.6	4.6	60.6	74.3	2.5
3.11	0.195	0.185	3.6	3.7	45.8	66.2	1.9
2.84	0.198	0.186	3.6	3.4	33.1	58.3	1.7
2.63	0.218	0.188	3.1	3.2	30.0	52.4	1.5
2.46	0.261	0.193	1.9	3.1	30.2	48.4	1.6
2.32	0.261	0.199	2.4	3.1	31.6	45.7	1.7
2.20	0.264	0.206	2.0	3.0	33.3	43.9	1.6
Overall		0.206	2.6	4.3	43.9	43.9	2.3

† Poss is the data completeness for the individual resolution shell. ‡ CumPoss is the cumulative completeness for the data set.

2.3. Neutron diffraction studies

The D_2O-soaked ecDHFR/MTX crystal was tested for neutron diffraction on the quasi-Laue LADI instrument

(λ = 3.5 Å, d$\lambda/\lambda \simeq 25\%$) at the ILL (Grenoble, France). This diffractometer uses a cylindrical neutron image-plate detector which completely surrounds the sample (Cipriani *et al.*, 1996; Myles *et al.*, 1998). LADI has been utilized for a number of successful protein neutron diffraction experiments (Habash *et al.*, 1997, 2000; Niimura *et al.*, 1997; Cooper & Myles, 2000; Coates *et al.*, 2001; Blakeley *et al.*, 2004). The ecDHFR–MTX crystal was exposed for 34 h per frame and a total of 21 frames were collected at two different crystal orientations. The φ separation between frames was typically 8°. All data were collected at 293 K. The data were indexed and integrated using the program *LAUEGEN* (Campbell *et al.*, 1998), which has been modified to account for the cylindrical geometry of the detector. The program *LSCALE* (Arzt *et al.*, 1999) was used to derive the wavelength-normalization curve using the intensity of symmetry-equivalent reflections measured at different wavelengths. The data were then scaled using the *SCALA* program within the *CCP*4 suite (Collaborative Computational Project, Number 4, 1994). A summary of the data-collection and scaling statistics is provided in Tables 1 and 2.

3. Results

We have collected a preliminary neutron diffraction data set in order to identify H-atom positions within the ecDHFR active-site residues, on the bound ligand MTX and of solvent molecules. Using ultrahigh-resolution X-ray diffraction at cryogenic temperatures (110 K or lower), highly precise macromolecular structures can be solved to atomic detail. However, H atoms only scatter X-rays weakly, causing ambiguities to arise upon inspection of electron-density maps for hydrogen peaks. Neutron diffraction can resolve this ambiguity, allowing precise positions of H (or D) atoms to be determined. However, to overcome limitations arising from the inherent low flux of the available neutron beams, crystal volumes of >1 mm^3 are usually required for adequate neutron diffraction and this makes the method quite prohibitive for many systems. The signal-to-noise ratio of the data can be improved by exchanging deuterium for hydrogen in the sample either by (i) growing or soaking the crystal in D_2O-based buffer (deuteration at chemically exchangeable positions) or (ii) forcing the expression organism (*i.e. E. coli*) to incorporate deuterated amino acids into the target protein at the biosynthetic level (deuteration at chemically non-exchangeable positions or perdeuteration). We report here initial neutron diffraction results from a D_2O-soaked ecDHFR–MTX crystal.

3.1. Preliminary neutron diffraction studies of D_2O-soaked ecDHFR–MTX crystals

The D_2O-soaked ecDHFR–MTX crystal diffracted neutrons to 2.2 Å resolution at room temperature on the LADI instrument at the ILL (Fig. 1). In the available beam time, we collected a partial data set in which the completeness within individual resolution shells dropped below 50% between 3.11 and 3.48 Å and the $I/\sigma(I)$ dropped below 2.0 around 2.46 Å. Reflections with $I/\sigma(I) > 2$ were observed beyond these limits and the cumulative completeness of the data set is 44% at 2.2 Å (Table 1). The ecDHFR–MTX crystal belongs to a high-symmetry space group ($P6_1$); consequently, our strategy involved collecting 13 images in 8° steps about the spindle rotation axis at one crystal setting and eight images at a second crystal orientation separated by a tilt of 20° in φ_y so as to record reflections in the 'blind zone'. The LADI instrument uses a limited quasi-Laue band pass (d$\lambda/\lambda \simeq 25\%$, λ = 3.5 Å) to maximize the flux at the sample. As a result, reflections that are stimulated at the extremes of the wavelength range are significantly weaker than those recorded at the peak incident spectrum (Fig. 2). Scale factors of up to 5 were required to normalize these reflections. The effective coverage of reciprocal space in each Laue diffraction pattern is dependent upon the wavelength range of neutrons in the incident spectrum that give rise to significantly recorded reflections. Thus, effective coverage is also sample-dependent. Clearly, for small weakly scattering crystals the effective

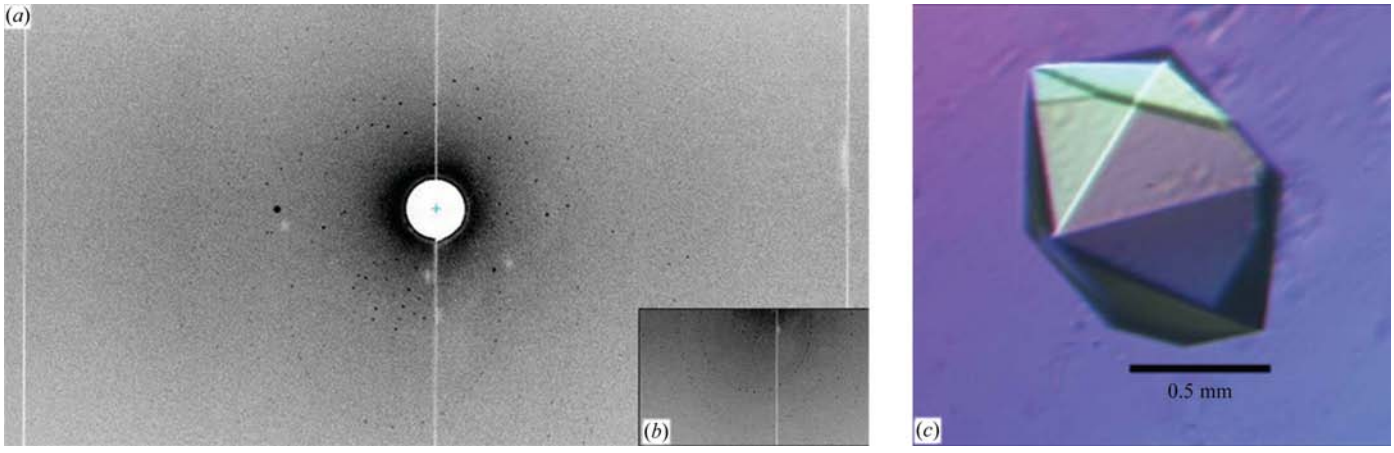

Figure 1
(*a*) Quasi-Laue neutron diffraction image from a 0.3 mm^3 D_2O-soaked DHFR–MTX crystal. (*a*) Laue diffraction pattern after a 34 h exposure. The highest resolution reflections extend to 2.2 Å. (*b*) A magnified section of the diffraction pattern containing reflections at ~2.5 Å. (*c*) The dimensions of the D_2O-soaked crystal are 1.4 × 1.0 × 0.3 mm or 0.3 mm^3.

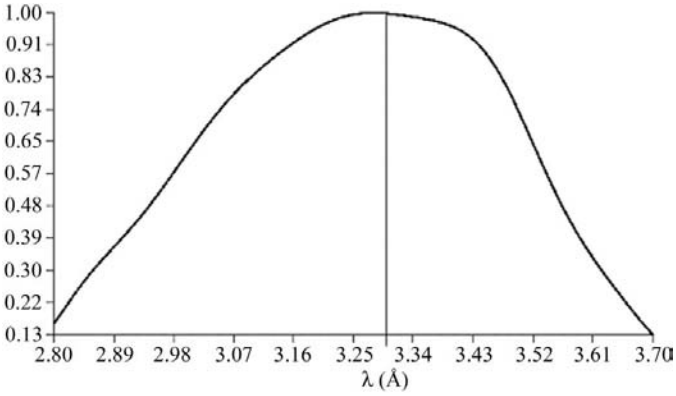

Figure 2
Wavelength-normalization curve determined by *LSCALE* (Arzt *et al.*, 1999). The *x* axis is the neutron wavelength used for diffraction. The *y* axis is an arbitrary scale for normalization and thus is dimensionless. The peak wavelength occurs at ∼3.3 Å and the intensity falls off towards either extreme of the graph at 2.8 and 3.7 Å, respectively.

experimental wavelength range used can be narrow and the φ rotation angle between images should be reduced accordingly to ensure that the 'recorded' regions of reciprocal space are truly contiguous.

4. Discussion

To our knowledge, the primitive unit-cell volume of the ecDHFR crystal (5.2×10^5 Å^3) is one of the largest so far investigated by high-resolution neutron crystallography. The ability to collect neutron diffraction data from a small H/D solvent-exchanged crystal that is only 0.3 mm^3 in volume is a consequence of the highly ordered lattice of the ecDHFR–MTX crystal. The solvent content of this crystal form is only 34.5% and we have been able to collect an ultrahigh-resolution X-ray data set from a native (H only) crystal. However, the relatively large unit-cell parameters of our crystal form ($a = b = 90.93$, $c = 72.36$ Å) combined with the broad wavelength band pass utilized ($d\lambda/\lambda = 25\%$) led to some spatially overlapped neutron reflections at higher resolution. The loss of these reflections contributes to the low data completeness, especially in the higher resolution shells.

Owing to the reduced data completeness, it is questionable whether D atoms can be modeled into the neutron density maps, even with the inclusion of the data that extend beyond the normal limit of around 3.1–3.4 to 2.2 Å. Previously, a neutron analysis of ConA at a similar resolution (2.75 Å) revealed that some H/D atoms could be modeled with confidence (Habash *et al.*, 1997). More recently, the same group has collected neutron diffraction data on D_2O-soaked ConA that extends the resolution to 2.4 Å; the authors attribute this improvement only to the H/D-exchange method and the longer duration for which the crystal was soaked in D_2O prior to neutron data collection (Habash *et al.*, 2000). The ConA data set to 2.75 Å was 75.5% complete; the ecDHFR–MTX data set extends to higher resolution but possesses much lower overall completeness (44% to 2.2 Å, 58% to 2.84 Å). Therefore, we are pursuing several strategies to overcome this problem.

Firstly, we are preparing fully deuterated DHFR protein and optimizing the growth of large-volume perdeuterated ecDHFR–MTX crystals for future neutron diffraction studies. The improved signal-to-noise ratio of neutron data collected from perdeuterated protein crystals (Shu *et al.*, 2000) will allow us to collect more complete and higher resolution data, even from comparably sized crystals. In order to reduce the density of reflections and the number of spatial overlaps on the LADI cylindrical detector, we will consider using a narrower wavelength band pass filter ($d\lambda/\lambda = 15\%$) and longer wavelength neutrons centered at $\lambda = 3.85$ Å for data collection. Whilst this strategy doubles the number of data frames required, the narrower $d\lambda/\lambda$ bandpass will reduce the experimental background and the use of perdeuterated crystals will deliver significant improvement in the signal-to-noise ratio of the data. Currently, we are analyzing the neutron density maps and performing subsequent rounds of structure refinement. The identification of enzyme and ligand protonation states as well as analysis of the H/D-exchange patterns will help deduce the catalytic mechanism and the inherent flexibility of ecDHFR, a catalytically efficient and well evolved enzyme (Fierke, Kuchta *et al.*, 1987) that is considered to be the 'progenitor' oxidoreductase (Kraut & Matthews, 1987).

BCB wishes to gratefully acknowledge the Joint Institute for Neutron Sciences at the University of Tennessee–Knoxville for the bestowing of a research fellowship for parts of the 2003–2004 and the 2004–2005 academic years. We thank ILL for the generous provision of neutron beam time on the LADI diffractometer. We would also like to thank Drs Anna Gardberg and Paul Langan for sharing their thoughtful insights.

References

Appleman, J., Howell, E., Kraut, J., Kuhl, M. & Blakley, R. (1988). *J. Biol. Chem.* **263**, 9187–9198.
Arzt, S., Campbell, J. W., Harding, M. M., Hao, Q. & Helliwell, J. R. (1999). *J. Appl. Cryst.* **32**, 554–562.
Bajorath, J., Kitson, D. H., Fitzgerald, G., Andzelm, J., Kraut, J. & Hagler, A. T. (1991). *Proteins*, **9**, 217–224.
Berman, H. M., Westbrook, J., Feng, Z., Gilliland, G., Bhat, T. N., Weissig, H., Shindyalov, I. N. & Bourne, P. E. (2000). *Nucleic Acids Res.* **28**, 235–242.
Blakeley, M. P., Kalb, A. J., Helliwell, J. R. & Myles, D. A. (2004). *Proc. Natl Acad. Sci. USA*, **101**, 16405–10610.
Bolin, J., Filman, D., Matthews, D., Hamlin, R. & Kraut, J. (1982). *J. Biol. Chem.* **257**, 13650–13652.
Bystroff, C., Oatley, S. J. & Kraut, J. (1990). *Biochemistry*, **29**, 3263–3277.
Campbell, J. W., Hao, Q., Harding, M. M., Nguti, N. D. & Wilkinson, C. (1998). *J. Appl. Cryst.* **31**, 496–502.
Cannon, W. R., Garrison, B. J. & Benkovic, S. J. (1997). *J. Mol. Biol.* **271**, 656–668.
Casarotto, M. G., Basran, J., Badii, R., Sze, K. H. & Roberts, G. C. (1999). *Biochemistry*, **38**, 8038–8044.
Chatake, T., Kurihara, K., Tanaka, I., Tsyba, I., Bau, R., Jenney, F. E. Jr, Adams, M. W. & Niimura, N. (2004). *Acta Cryst.* D**60**, 1364–1373.

Chen, Y. Q., Kraut, J., Blakley, R. L. & Callender, R. (1994). *Biochemistry*, **33**, 7021–7016.
Chen, Y. Q., Kraut, J. & Callender, R. (1997). *Biophys. J.* **72**, 936–941.
Cipriani, F., Castagna, J. C., Wilkinson, C., Oleinek, P. & Lehmann, M. S. (1996). *J. Neutron Res.* **4**, 79–85.
Coates, L., Erskine, P. T., Wood, S. P., Myles, D. A. & Cooper, J. B. (2001). *Biochemistry*, **40**, 13149–13157.
Cocco, L., Groff, J., Temple, C. Jr, Montgomery, J., London, R., Matwiyoff, N. & Blakley, R. (1981). *Biochemistry*, **20**, 3972–3978.
Cocco, L., Roth, B., Temple, C. Jr, Montgomery, J., London, R. & Blakley, R. (1983). *Arch. Biochem. Biophys.* **226**, 567–577.
Collaborative Computational Project, Number 4 (1994). *Acta Cryst.* D**50**, 760–763.
Cooper, J. B. & Myles, D. A. (2000). *Acta Cryst.* D**56**, 246–248.
Fierke, C. A., Johnson, K. A. & Benkovic, S. J. (1987). *Biochemistry*, **26**, 4085–4092.
Fierke, C. A., Kuchta, R. D., Johnson, K. A. & Benkovic, S. J. (1987). *Cold Spring Harbor Symp. Quant. Biol.* **52**, 631–638.
Greatbanks, S. P., Gready, J. E., Limaye, A. C. & Rendell, A. P. (1999). *Proteins*, **37**, 157–165.
Habash, J., Raftery, J., Nuttall, R., Price, H., Wilkinson, C., Kalb (Gilboa), A. J. & Helliwell, J. (2000). *Acta Cryst.* D**56**, 541–550.
Habash, J., Raftery, J., Weisgerber, S., Cassetta, A., Lehmann, M. S., Hoghoj, P., Wilkinson, C., Campbell, J. & Helliwell, J. R. (1997). *J. Chem. Soc. Faraday Trans.* **93**, 4313–4317.
Hanson, B. L., Langan, P., Katz, A. K., Li, X., Harp, J. M., Glusker, J. P., Schoenborn, B. P. & Bunick, G. J. (2004). *Acta Cryst.* D**60**, 241–249.
Hood, K. & Roberts, G. C. (1978). *Biochem. J.* **171**, 357–366.
Howell, E. E., Villafranca, J. E., Warren, M. S., Oatley, S. J. & Kraut, J. (1986). *Science*, **231**, 1123–1128.
Huennekens, F. M. (1994). *Adv. Enzyme Regul.* **34**, 397–419.
Huennekens, F. M. (1996). *Protein Sci.* **5**, 1201–1208.
Jancarik, J. & Kim, S.-H. (1991). *J. Appl. Cryst.* **24**, 409–411.
Kraut, J. & Matthews, D. A. (1987). *Biological Macromolecules and Assemblies*, edited by F. A. Jurnak & A. McPherson, pp. 1–71. New York: John Wiley & Sons.
Kurihara, K., Tanaka, I., Chatake, T., Adams, M. W., Jenney, F. E. Jr, Moiseeva, N., Bau, R. & Niimura, N. (2004). *Proc. Natl Acad. Sci. USA*, **101**, 11215–11220.
London, R. E., Howell, E. E., Warren, M. S., Kraut, J. & Blakley, R. L. (1986). *Biochemistry*, **25**, 7229–7235.
Matthews, D. A., Alden, R. A., Bolin, J. T., Freer, S. T., Hamlin, R., Xuong, N., Kraut, J., Poe, M., Williams, M. & Hoogsteen, K. (1977). *Science*, **197**, 452–455.
Matthews, D. A., Bolin, J. T., Burridge, J. M., Filman, D. J., Volz, K. W., Kaufman, B. T., Beddell, C. R., Champness, J. N., Stammers, D. K. & Kraut, J. (1985). *J. Biol. Chem.* **260**, 381–391.
Miller, G. & Benkovic, S. (1998). *Biochemistry*, **37**, 6336–6342.
Miller, G., Wahnon, D. & Benkovic, S. (2001). *Biochemistry*, **40**, 867–875.
Myles, D. A., Bon, C., Langan, P., Cipriani, F., Castagna, J. C., Lehmann, M. S. & Wilkinson, C. (1998). *Physica B*, **241–243**, 1122–1130.
Niimura, N., Minezaki, Y., Nonaka, T., Castagna, J. C., Cipriani, F., Hoghoj, P., Lehmann, M. S. & Wilkinson, C. (1997). *Nature Struct. Biol.* **4**, 909–914.
Ostermann, A., Tanaka, I., Engler, N., Niimura, N. & Parak, F. G. (2002). *Biophys. Chem.* **95**, 183–193.
Ozaki, Y., King, R. & Carey, P. (1981). *Biochemistry*, **20**, 3219–325.
Poe, M., Greenfield, N., Hirshfield, J., Williams, M. & Hoogsteen, K. (1972). *Biochemistry*, **11**, 1023–1030.
Reyes, V. M., Sawaya, M. R., Brown, K. A. & Kraut, J. (1995). *Biochemistry*, **34**, 2710–2723.
Sawaya, M. & Kraut, J. (1997). *Biochemistry*, **36**, 586–603.
Schnell, J., Dyson, H. & Wright, P. (2004). *Annu. Rev. Biophys. Biomol. Struct.* **33**, 119–140.
Schoenborn, B. & Knott, R. (1996). *Basic Life Sciences*, p. 452. New York: Plenum.
Shu, F., Ramakrishnan, V. & Schoenborn, B. P. (2000). *Proc. Natl Acad. Sci. USA*, **97**, 3872–3877.
Stone, S. & Morrison, J. (1988). *Biochemistry*, **27**, 5493–5499.
Taira, K., Chen, J.-T., Mayer, R. & Benkovic, S. J. (1987). *Bull. Chem. Soc. Jpn*, **60**, 3017–3024.
Tuominen, V. U., Myles, D. A., Dauvergne, M. T., Lahti, R., Heikinheimo, P. & Goldman, A. (2004). *Acta Cryst.* D**60**, 606–609.
Villafranca, J. E., Howell, E. E., Voet, D. H., Strobel, M. S., Ogden, R. C., Abelson, J. N. & Kraut, J. (1983). *Science*, **222**, 782–788.
Zeig, J., Maples, V. & Kushner, S. (1978). *J. Bacteriol.* **134**, 958–966.